CFD Letters

Journal homepage:
https://semarakilmu.com.my/journals/index.php/CFD_Letters/index
ISSN: 2180-1363

Power Prediction of Tandem Wind Rotor: Applied on Different Climatic Zones

Nasreddine Akermi[1,*], Mohamed Reda Ahmed Bacha[2], Ali Benouar[2], Azzeddine Khorsi[2]

[1] Mechanical Department, Faculty of Applied Sciences, University of Ibn Khaldoun, BP P 78 Zaaroura 14000, Tiaret , Algeria
[2] Laboratory of complex systems (LCS), Higher School of Electrical and Energy Engineering ESGEE, Oran, Algeria

ARTICLE INFO

Article history:
Received 5 September 2022
Received in revised form 8 October 2022
Accepted 9 November 2022
Available online 1 April 2023

Keywords:
Nouadhibou; Tiaret; performance; H-Darrieus; power; three-bladed; tandem; lift; torque

ABSTRACT

The present study highlights a comparative numerical simulation of two geometric configurations of a three-bladed vertical axis wind rotor. The simulation was carried out for different wind speeds of the last year 2021 and applied on different climatic zones, Tiaret from Algeria and Nouadhibou from Mauritania. This simulation is useful to estimate the aerodynamic power of a new three-bladed tandem (biplane) geometry. The objective of this study is to predict the lift and the power coefficients in order to estimate the efficiency, according to the blades active surfaces of the two designs, monoplane three-bladed and three-bladed in tandem configurations. The results obtained by the simulation show relatively a significant agreement with the experiences and the 6DOF approach published previously. The efficiency of the tandem rotor is higher than the monoplane three-bladed rotor (Cp_{max} = 0.46). The climatic zone of Nouadhibou (Mauritania) is the windiest during the year 2021 referring to the variation of the average measured wind speeds comparing to Tiaret zone. The installation of this new type of design at the zone of Nouadhibou is preferable in terms of the highest produced aerodynamic power.

1. Introduction

Energy has always been necessary for the continuity of humanity, in particular, basic needs like food and the daily man activities. Therefore, human requirements for fossil energy sources have become greater due to the industrial revolution. However, the high rate of consumption, which depends mainly on available fossil resources relatively, increases carbon emissions, MULLER, O. *et al.,* [1]. These emissions decreased slightly by 6% in 2020 due to the contraction of industrial activities during the period of the COVID19 pandemic, as well as, the gradual return to renewable energy sources.

Due to the global health and political crises influencing rising fuel costs, as well as, the environmental effects, developing countries are moving towards intelligent management of urban areas through the construction of buildings equipped with positive sources, Rajeanderan R. *et al.,* [2].

* *Corresponding author.*
E-mail address: nasreddine.akermi@gmail.com (Nasreddine Akermi)

https://doi.org/10.37934/cfdl.15.4.8091

Currently, wind turbines installed in urban areas have become promising to compensate the acute shortage of power plants, Hau, E. *et al.,* [3].

The vertical axis wind turbines VAWT is the most useful in urban areas because of its simplicity and its adaptation with the random velocity direction. Anemometers installed on the buildings roofs over a specific time range may measure the wind speed correctly, Nofirman F. *et al.,* [4].

Several years ago, many investigations were carried out in order to estimate and develop the production capacities of different configurations of the vertical axis wind turbines design.

Numerical investigation of Dominy, R. G. *et al.,* [5] confirms that the self-starting of a three-bladed rotor is technically possible comparing to a two-bladed rotor for stationary wind speed. If the wind turbine reaches its operating optimal mode, the aerodynamic power produced will be independent of the solidity and the tip speed ratio TSR becomes invariant, explaining the causes of the inability of low solidity fixed pitch vertical axis wind turbines and the features to aid self-starting. Rezaeiha, A. *et al.,* [6]. The numerical investigation carried out by Kaufmann, K *et al.,* [7]. Expresses the relationship between the wing span direction and the dynamic stall vortex formation. Islam, M. *et al.,* [8] have tested several numerical models, which have already been used to predict the performances of vertical axis wind turbines, in particular the conception of H-Darrieus rotors prototypes.

Kooiman, S.J. *et al.,* [9] Express that the aerodynamic performances of vertical axis wind turbines are independent of the direction of the field of fluctuating speeds, nevertheless, its effect is quantifiable. The paper of Ashwindran, S. *et al.,* [10] studied the sensitivity of the quality of the sliding mesh and the effect of the turbulence model, as well as, the choice of the time step including the aerodynamic forces. Ramirez, D.A *et al.,* [11] carried out the design and the hydrodynamic analysis of a Darrieus vertical axis wind turbine of 500 W, for a free flow speed of 1.5 m/s used for the blades design. A range of experimental and numerical assessment of airfoil polar for use in Darrieus wind turbines carried out by Bianchini, A. *et al.,* [12]. The results show a higher lift coefficient at stall, and should be taken with NACA 0018 data comparing to data from experiments of Sheldahl *et al.,* [13]. The newest optimization carried out by Palanisamy Mohan Kumar *et al.,* [14] consists of design and construction of vertical axis Darrieus type micro wind turbine and shed additional light on sensor and data acquisition. Edwards, J. M. *et al.,* [15] study in their paper the different aerodynamic performance of a small-scale vertical axis wind turbine VAWT by new experimental methods.

The comparative numerical study carried out by AKERMI *et al.,* [16] focuses on the unsteady numerical analysis of the 6DOF approach, and shown that the two-blade design does not achieve higher specific speeds according to the wind speed (TSR ≤ 4), due to their structural and aerodynamic limitations. Enderaaj S. *et al.,* [17] tried to optimize a Vertical axis wind rotor Solidity applied for Cooling Tower configuration. The results of comparative analysis of Wind speeds in Northeastern of Thailand developed by Natthapat Pawintanathon *et al.,* [18] shown that the economic investment depends on wind energy potentials of different region.

The results of the comparative study made by Perry Roth-Johnson *et al.,* [19] of the biplane wind rotor show that this design is attractive for large blades.

Several experimental tests have been carried out by Rodríguez-Sevillano, Á.A *et al.,* [20] in wind tunnel on the biplane configuration in order to evaluate their aerodynamic performances; the results obtained have been useful in micro air vehicles.

The present investigation focuses on the effect of the wind speed variation at the produced aerodynamic power. The estimated power coefficients are useful to carry out a Comparative study of the performances, the efficiency, and the aerodynamic effect of the blades active areas variation to the monoplane three-bladed wind rotor configuration, as well as, the new proposed biplane three-bladed design.

This numerical study is applied on two climatic zones; the region of Tiaret from Algeria, the other is Nouadhibou from Mauritania, for the last year 2021 [weather spark platform 2021].

2. Methodology

2.1 Aerodynamic Performances:

The air profile immersed in airflow can be subjected to various aerodynamic forces. These forces cause a slowing due to the tangential friction with the body surface or normal lifting forces as shown in Figure 1.

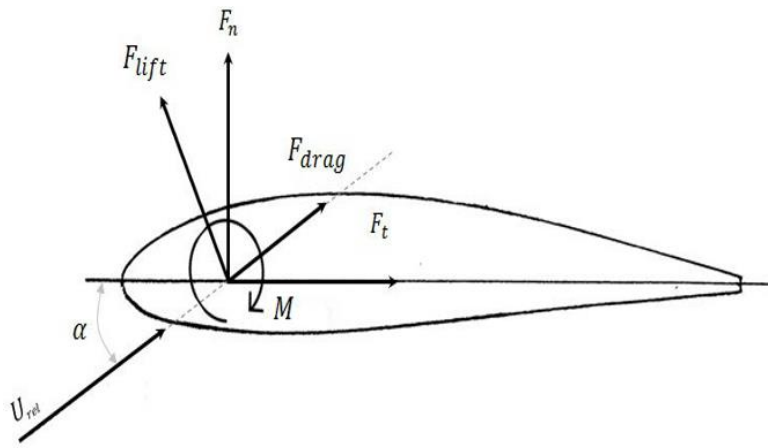

Fig. 1. Aerodynamic performances

The tip speed ratio defined as:

$$TSR = \frac{\omega R}{U_\infty} \tag{1}$$

where the tip speed ratios, TSR, rotor radios, R, Angular velocity, ω, Inlet velocity, U_∞

The power coefficient corresponds to the efficiency and aerodynamic performances of a wind turbine. It is the ratio between the power available in the wind and the power developed by the rotor (limit of Betz).

$$C_p = \frac{P}{P_a} = \frac{P}{\frac{1}{2}.\rho.A.U_\infty^3} \tag{2}$$

where the power coefficient, C_p, Swept area, A, Air density, ρ, Aerodynamic power, P

The torque coefficient is defined by the ratio between the power coefficient and the specific speed.

$$C_q = \frac{C_p}{TSR} \tag{3}$$

where the torque coefficient, C_q

The solidity factor is defined by geometrical ratio of the chord length, number of blades and the rotor radios:

$$\sigma = \frac{N.C}{D} \tag{4}$$

where the solidity, σ, Blades number, N, Blade chord length C, Rotor diameter, D

Reynolds number is based on a relationship between the free stream velocity and the speed ratio

$$\mathrm{R}_e = \frac{\omega.R.C}{\nu} \tag{5}$$

where the Reynolds number, R_e, Kinematic viscosity, ν

The nominal power is defined according the swept section, as well as, the materials used for the construction of the rotor, the nominal velocity can be can be defined empirically by the relationship [18].

$$U_N = 1.5\ U_\infty \tag{6}$$

where the nominal velocity, $\mathrm{U_N}$

2.2 Unsteady Modeling of Turbulent Flow

Turbulent flows are governed by Navier-Stockes equations that are established according to the components ($\mathrm{u_i}$,$\mathrm{u_j}$) and the fluid pressure:

Continuity

$$\frac{\partial \rho}{\partial t} + \frac{\partial}{\partial x_i}(\rho u_i) = 0 \tag{7}$$

Momentum conservation

$$\frac{\partial \rho}{\partial t}(\rho u_i) + \frac{\partial}{\partial x_j}\left(\rho u_i u_j\right) = \frac{\partial}{\partial x_j}\left(-\rho \delta_{ij} + \tau_{ij}\right) \tag{8}$$

2.3 Implemented Climatic Zones

This section deals with the extended hourly mean wind vector (speed and direction) at 10 meters above the ground.

The average hourly wind speed in Nouadhibou and Tiaret experiences significant seasonal variation over the course of the year. Table 1. Shows the variation of the average wind speed during the 2021 year.

Table 1
Wind velocity during the last year 2021 [Weather spark 2021]

Months	Wind velocities m/s Nouadhibou (Mauritania)	Wind velocities m/s Tiaret (Algeria)
December	5,75	4,36
January	6.03	4,42
February	6,33	4,22
March	7,14	4,22
April	7,69	3,86
May	7,75	3,58
June	6,72	3,47
July	6,14	3,44
August	6.36	3,53
September	6.08	3,78
October	5.44	4,25
November	5.39	4,42

2.4 Experimental Validation

The computation area chord length is C=1m. Figure 2 Shows that two-dimensional average steady inlet velocity has been introduced. Air-air interface condition defines the adjacent areas (fixed and rotating area).

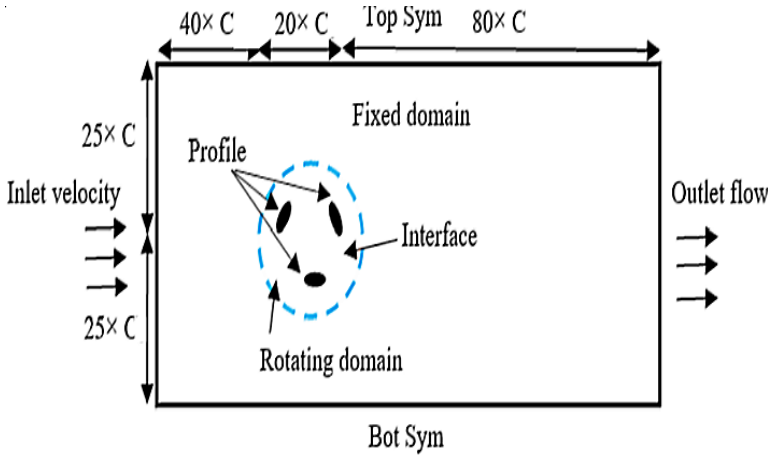

Fig. 2. Calculation domains

Several grids of the vertical wind rotor have been generated and tested including the calculation convergence criteria and experimental validation for the two-bladed and three-bladed configurations.

The number of 2D hexahedral elements counts approximately 450,000 and 270,000 successively. The numerical investigation was carried out at the Ansys V 17.1 Fluent code using parallel calculation: Intel Core i5 3.10 GHz processor computing machine, 4 GB of RAM, 64 bits. Figure 3 shows the quality of generated mesh.

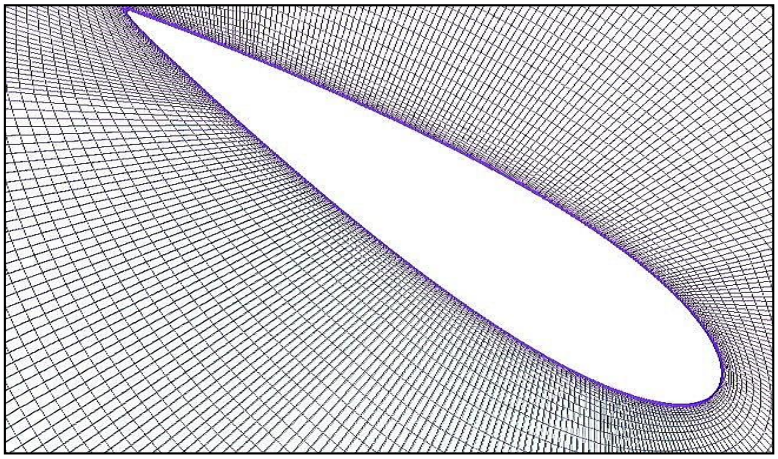

Fig. 3. Mesh quality

Table 2 Resumes the technical characteristics of vertical axis wind rotor prototype.

Table 2
Wind turbine prototype datasheet

Technical specifications	values
Nominal power	10 Kw
operational wind velocity	3 m/s
Allowable wind velocity	20 m/s
Rotor height	14 m
Rotor area	68 m^2

2.5 Tip Speed Ratio (TSR) Choice

Figure 4 indicates the results of numerical computation carried out on the two configurations by the 6DOF approach. the results shown express that the specific speed TSR = 4 represents the optimum operation mode for the two and three vertical axis bladed rotors at a wind speed equal or less than 10 m/s.

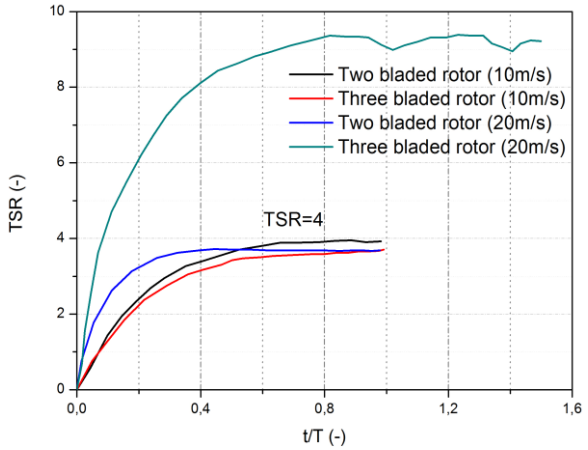

Fig. 4. Tip speed ratio vs time report [16]

3. Results

3.1 Results Validation

Figure 5 shows the variation of the lift force coefficient C_l according to the rotor angle. The results obtained by the unsteady k-ω SST model express a good agreement with those obtained experimentally by Sheldahl *et al.,* [13] and Alessandro *et al.,* [12], However, an overestimation of the lift force has been noticed at 20° angular position comparing to the experimental results and the 6DOF approach.

Even so, the unsteady k-ω SST model shown its efficiency during the simulation by the good prediction of aerodynamic stall, justified by the drop lift force at the azimuthal position θ ≈12 °.

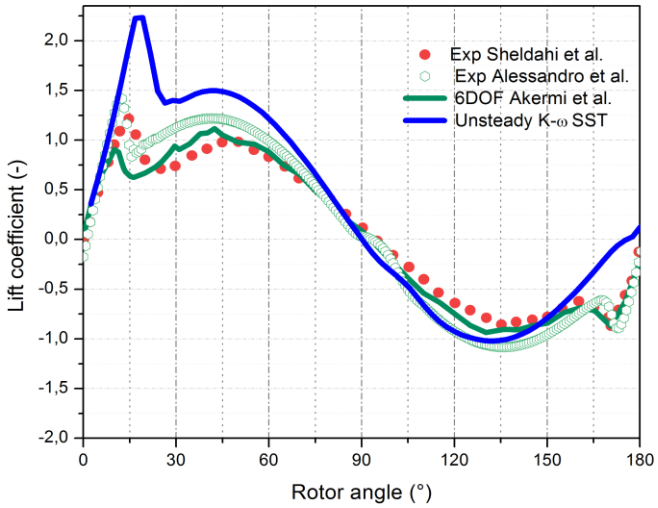

Fig. 5. Lift coefficient vs rotor angle

3.2 Tandem (Biplane) Concept

The concept of the biplane as shown in Figure 6 and Figure 7 was first used in the early days of aviation, when engines were heavy, not very powerful and with low flight speed. Therefore, it needed a large wing area to provide lift [18].

The formula of the biplane is summarized in two wings of often-equal span, placed one above the other. This concept is frequently applied on horizontal axis wind turbines but remains promising for vertical axis wind rotors, particularly, in urban areas.

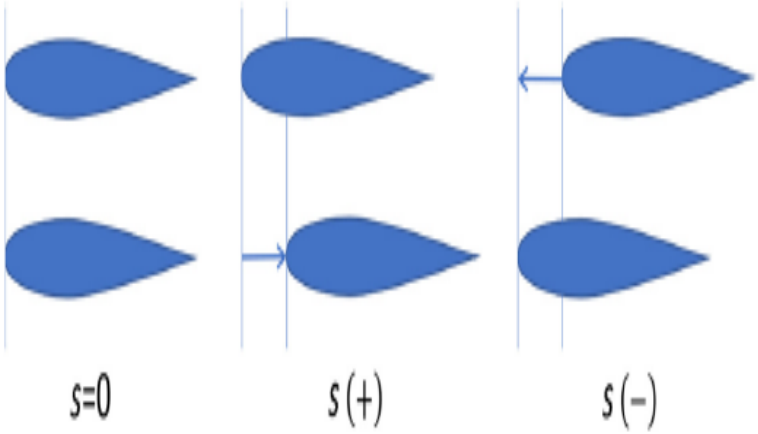

Fig. 6. Aerofoils Tandem stagger [20]

Fig. 7. Aerofoils in Tandem

3.3 Grid Generation

Figure 8 below represents the generated grid of the three-bladed tandem vertical wind rotor. Where, the two blades of the biplane are displaced (Stagger)of 0, 5 * Chord Downstream shift and spaced vertically by 1 * chord. The generated grid consists of two calculation domains, once rotating and the other fixed, ensuring the boundary conditions. The total number of the 3D hexahedral elements is 329000.

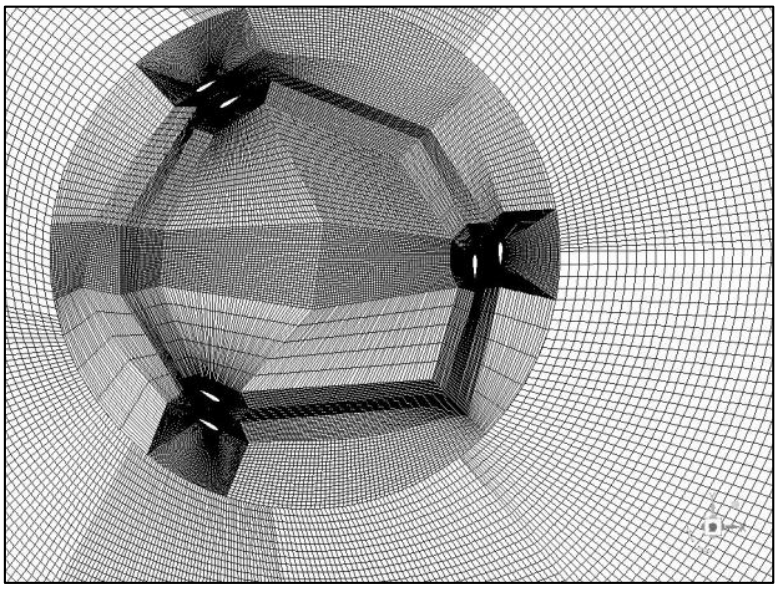

Fig. 8. Three bladed Tandem H-Darrieus wind rotor grid

3.4 Lift Coefficient Results

As shown in Figure 9 the lift coefficient results obtained have been compared to the experiences published previously.

The results show a relative agreement with an important lift drop in the angular interval [100, 120°], comparing to the experimental values, which can be justified by the high solidity (number of blades) of the three-bladed geometry compared to the two-bladed one, as well as, the high wind inlet velocity introduced for the lift coefficient prediction (Nouadhibou, V=7.75m/s).

The results validation faced the limitation of preliminary experiments and investigations for this new proposed type of wind turbine configuration, especially the three-bladed tandem wind rotor.

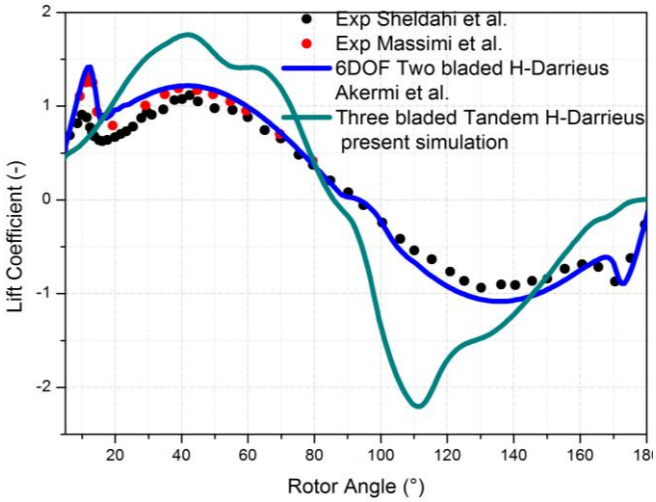

Fig. 9. Lift coefficient validation

Figure 10 expresses that the maximum value of lift coefficient is higher for the Tandem configuration comparing to the monoplane three-blade configuration C_l=2.25 at the azimuth angle θ = 110° (Nouadhibou climatic zone).

The maximum lift value is highest for the Tandem configuration comparing to the monoplane three-blade configuration C_l=1.8 at the azimuth angle θ = 45° (Tiaret climatic zone) as shown in Figure 11.

The numerical results obtained show that the lift is proportional to the inlet wind velociy for the two climatic zones (V_{max}=7.75 m/s for Nouadhibou zone and V_{max}=4.42 m/s for Tiaret climatic zone).

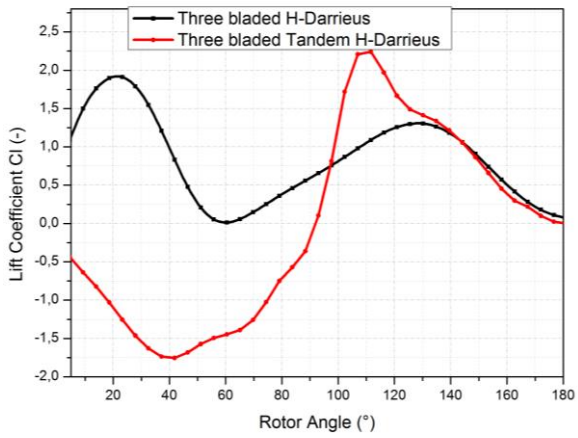

Fig. 10. Lift coefficient for the climatic zone of Nouadhibou from Mauritania

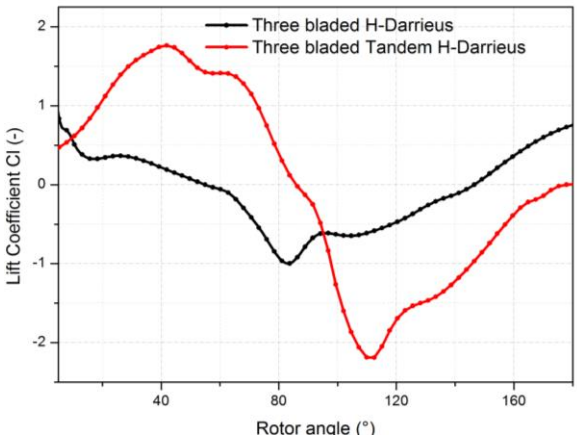

Fig. 11. Lift coefficient for the climatic zone of Tiaret from Algeria

3.5 Power Coefficient Results

The results shown in Figures 12 and Figure 13 confirm that the efficiency of the Tandem wind rotor is higher than the monoplane three-bladed rotor for the two climatic zones Nouadhibou and Tiaret probably due to the increase of the blades active areas (C_{pmax}= 0.46 and 0.26 successively).

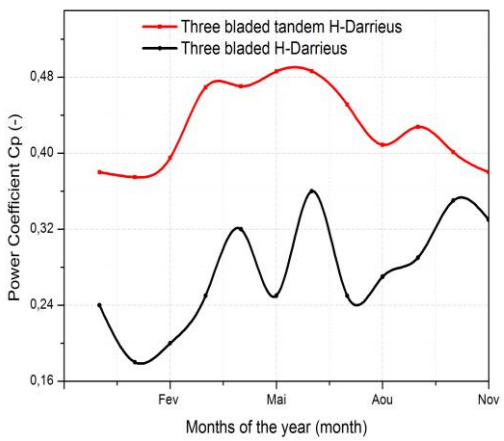

Fig. 12. Power coefficient for the climatic zone of Nouadhibou from Mauritania

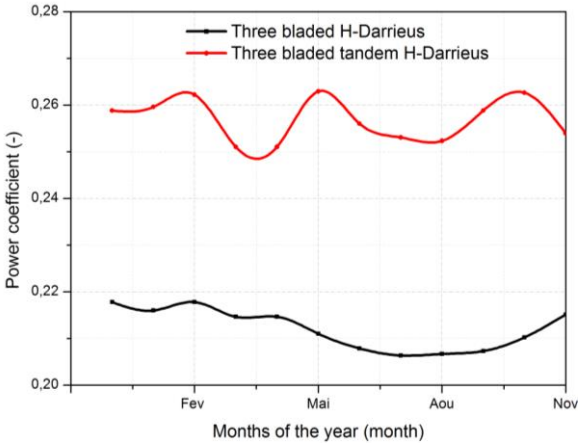

Fig. 13. Power coefficient for the climatic zone of Tiaret from Algeria

3.6 Velocity and Pressure Contours of Three Blade Tandem Rotor (V_{max} = 7.75 m/s)

The specific speed (TSR) taken into account for the prediction of the power coefficient is λ=4 depending on the optimal operating mode of the vertical wind aerogenerators.

The velocity and the static pressure contours shown in Figures 14 and Figure 15 successively indicate a significant acceleration of the flow on the extrados part of the Tandem blades comparing to the monoplane three-bladed configuration due to the low-pressure areas.

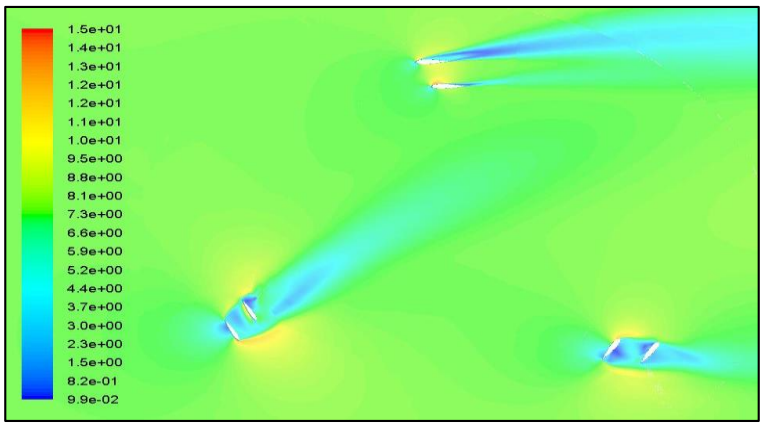

Fig. 14. Velocity contours (V_{max} = 7.75 m/s)

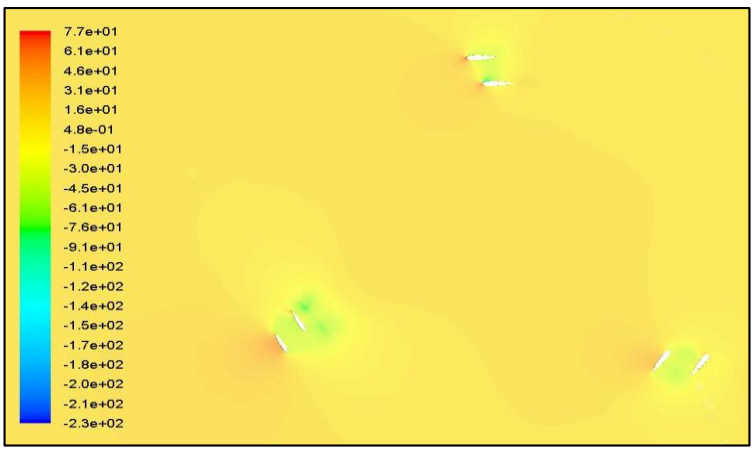

Fig. 15. Static pressure contours (V_{max} = 7.75 m/s)

4. Conclusions

The present work focuses on a comparative numerical investigation of two geometric configurations of vertical wind rotors, monoplane three-blade type and the three-blade Tandem design or biplane.

The comparative study is basing primarily on the aerodynamic performances of the two configurations studied. The lift force generated by the Tandem wind-blades interaction is greater than the monoplane configuration due to the double active surface subjected to the lift force.

The estimated power of the tandem wind turbine is the highest (C_{pmax}=0.48) in particular for the windy climatic zone of Nouadhibou, wind speed exceeds 7.75 m/s.

The main defect noted after interpretation of the numerical results obtained for the Tandem configuration is the possibility of an important aerodynamic braking during the rotation of the blades, probably due to the aerodynamic wake generated by the interaction of the blades in tandem with the wind at the inlet of the wind rotor comparing to the monoplane three-blade rotor.

The present study will be followed by several parametric investigations, depending on the relationship between the angle of attack and the pitch angle with the aerodynamic performances, as well as the possibility of self-starting of this new configuration. The prediction of the aerodynamic characteristics can be improved by the 6DOF approach introducing the mass properties of the Tandem rotor.

Acknowledgement
The authors would like to acknowledge everyone who has contributed to this work. Especially, the staff of mechanical department at the University of Ibn Khaldoun, as well as, the members of the Laboratory of Complex Systems LCS including the research team OSEC for their support and scientific vision. “This research was not funded by any grant”.

References

[1] Muller, Olivier, Herve Chung, Pauline Bricker, and Roxane Laroche. "Climate Change and Electricity, European carbon factor, Benchmarking of CO 2 emissions by Europe's largest electricity utilities-December 2020." (2020).

[2] Revichandran, Rajeanderan, Jaffar Syed Mohamed Ali, Moumen Idres, and A. K. M. Mohiuddin. "Energy Efficiency and Optimization of Buildings for Sustainable Development in Malaysia." *Journal of Advanced Research in Fluid Mechanics and Thermal Sciences* 93, no. 2 (2022): 28-36. https://doi.org/10.37934/arfmts.93.2.2836

[3] Hau, Erich, and Horst von Renouard. *Wind turbines: fundamentals, technologies, application, economics*. New York: Springer, 2003.

[4] Firdaus, Nofirman, Bambang Teguh Prasetyo, Hasnida Ab-Samat, Heri Suyanto, and Rusjdi Halim. "Wind Energy Potential on A Highrise Building: A Preliminary Study." *Journal of Advanced Research in Fluid Mechanics and Thermal Sciences* 88, no. 3 (2021): 20-30. https://doi.org/10.37934/arfmts.88.3.2030

[5] Dominy, Robert, P. Lunt, A. Bickerdyke, and J. Dominy. "Self-starting capability of a Darrieus turbine." *Proceedings of the Institution of Mechanical Engineers, Part A: Journal of Power and Energy* 221, no. 1 (2007): 111-120. https://doi.org/10.1243/09576509JPE340

[6] Rezaeiha, Abdolrahim, Hamid Montazeri, and Bert Blocken. "Towards optimal aerodynamic design of vertical axis wind turbines: Impact of solidity and number of blades." *Energy* 165 (2018): 1129-1148. https://doi.org/10.1016/j.energy.2018.09.192

[7] Kaufmann, Kurt, Christoph B. Merz, and Anthony D. Gardner. "Dynamic stall simulations on a pitching finite wing." *Journal of Aircraft* 54, no. 4 (2017): 1303-1316. https://doi.org/10.2514/1.C034020

[8] Islam, Mazharul, David S-K. Ting, and Amir Fartaj. "Aerodynamic models for Darrieus-type straight-bladed vertical axis wind turbines." *Renewable and sustainable energy reviews* 12, no. 4 (2008): 1087-1109. https://doi.org/10.1016/j.rser.2006.10.023

[9] Kooiman, S. J., and S. W. Tullis. "Response of a vertical axis wind turbine to time varying wind conditions found within the urban environment." *Wind Engineering* 34, no. 4 (2010): 389-401. https://doi.org/10.1260/0309-524X.34.4.389

[10] Ashwindran, S., A. A. Azizuddin, and A. N. Oumer. "Computational fluid dynamic (CFD) of vertical-axis wind turbine: mesh and time-step sensitivity study." *Journal of Mechanical Engineering and Sciences* 13, no. 3 (2019): 5604-5624. https://doi.org/10.15282/jmes.13.3.2019.24.0450

[11] Ramirez, D., A. Rubio-Clemente, and E. Chica. "Design and numerical analysis of an efficient H-Darrieus vertical-axis hydrokinetic turbine." *Journal of Mechanical Engineering and Sciences* 13, no. 4 (2019): 6036-6058. https://doi.org/10.15282/jmes.13.4.2019.21.0477

[12] Bianchini, Alessandro, Francesco Balduzzi, John M. Rainbird, Joaquim Peiro, J. Michael R. Graham, Giovanni Ferrara, and Lorenzo Ferrari. "An Experimental and Numerical Assessment of Airfoil Polars for Use in Darrieus Wind Turbines: Part 2—Post-Stall Data Extrapolation Methods." In *Turbo Expo: Power for Land, Sea, and Air*, vol. 56802, p. V009T46A007. American Society of Mechanical Engineers, 2015. https://doi.org/10.1115/1.4031270

[13] Sheldahl, R. E., and P. C. Klimas. "Aerodynamic characteristics of seven airfoil sections through 180 degrees of attack for use in aerodynamic analysis of vertical axis wind turbines, SAND80-2114." *Sandia National Laboratories, Albuquerque, NM* (1981). https://doi.org/10.2172/6548367

[14] Kumar, P. M., S. Anbazhagan, N. Srikanth, and T. C. Lim. "Optimization, design, and construction of field test prototypes of adaptive hybrid Darrieus turbine." *J Fundam Renewable Energy* 7, no. 245 (2017). https://doi.org/10.4172/2090-4541.1000245

[15] Edwards, Jonathan M., Louis Angelo Danao, and Robert J. Howell. "Novel experimental power curve determination and computational methods for the performance analysis of vertical axis wind turbines." *Journal of Solar Energy Engineering* 134, no. 3 (2012). https://doi.org/10.1115/1.4006196

[16] Akermi, N. Khorsi, A. and Imine O. "Numerical Study of H-Darrieus wind turbine Start-up by Six degrees of Freedom Model." *International Review of Mechanical Engineering* 13, (2019): 235-241. https://doi.org/10.15866/ireme.v13i4.16786

[17] Roth-Johnson, Perry, and Richard E. Wirz. "Aero-structural investigation of biplane wind turbine blades." *Wind Energy* 17, no. 3 (2014): 397-411. https://doi.org/10.1002/we.1583

[18] Singh, Enderaaj, Sukanta Roy, Yam Ke San, and Law Ming Chiat. "Optimisation of H-Darrieus VAWT Solidity for Energy Extraction in Cooling Tower Exhaust Systems." *Journal of Advanced Research in Fluid Mechanics and Thermal Sciences* 91, no. 2 (2022): 51-61. https://doi.org/10.37934/arfmts.91.2.5161

[19] Pawintanathon, Natthapat, Somchai Saeung, and Juntakan Taweekun. "Techno-Economic Analysis of Wind Energy Potential in North-Eastern of Thailand." *Journal of Advanced Research in Fluid Mechanics and Thermal Sciences* 93, no. 1 (2022): 25-49. https://doi.org/10.37934/arfmts.93.1.2549

[20] Rodríguez-Sevillano, Ángel Antonio, Miguel Ángel Barcala-Montejano, Rafael Bardera-Mora, Adelaida García-Magariño García, María Elena Rodríguez-Rojo, Sara Morales-Serrano, and Jaime Fernández-Antón. "Selection Criteria for Biplane Wing Geometries by Means of 2D Wind Tunnel Tests." *Applied Mechanics* 3, no. 2 (2022): 628-648. https://doi.org/10.3390/applmech3020037